Turkish Journal of Chemistry
http://journals.tubitak.gov.tr/chem/
Research Article

Turk J Chem
(2015) 39: 576 – 588

doi:10.3906/kim-1412-15

Fabrication of silver nanoparticles in poly (N-isopropylacrylamide-co-allylacetic acid) microgels for catalytic reduction of nitroarenes

Zahoor H. FAROOQI[1,*], Naghza TARIQ[1], Robina BEGUM[2], Shanza Rauf KHAN[1], Zafar IQBAL[3], Abbas KHAN[4]
[1]Institute of Chemistry, University of the Punjab, Lahore, Pakistan
[2]Centre for Undergraduate Studies, University of the Punjab, Lahore, Pakistan
[3]Department of Chemistry, Quaid-i-Azam University, Islamabad, Pakistan
[4]Department of Chemistry (Shankar Campus), Abdul Wali Khan University, Mardan, Pakistan

Received: 09.12.2014 • **Accepted/Published Online:** 15.02.2015 • **Printed:** 30.06.2015

Abstract: Poly(N-isopropylacrylamide-co-allyl acetic acid) [p(NIPAM-co-AAAc)] microgels were synthesized in aqueous medium by free radical emulsion polymerization using N-isopropylacrylamide as monomer, allylacetic acid as comonomer, and N,N-methylene-bis-acrylamide as cross-linker. Silver nanoparticles were fabricated inside the microgels by in situ reduction of silver ions. Microgels were analyzed by UV-visible spectroscopy, FTIR, XRD, TEM, and DLS. The formation of silver nanoparticles was confirmed by UV-visible spectroscopy. UV-visible spectra of the Ag-poly(N-isopropylacrylamide-co-allyl acetic acid) hybrid microgels showed a prominent absorption peak at about 411 nm. This peak was due to the surface plasmon resonance effect of silver nanoparticles. The hybrid microgels were used as catalyst for the reduction of nitroarenes. The reduction reactions were found to be first order with respect to nitroarenes with the values of apparent rate constant (k_{app}) equal to 0.248, 0.215, and 0.089 min^{-1} for 4-nitrophenol, 4-nitroaniline, and nitrobenzene respectively at 27 °C in aqueous medium. Silver nanoparticles were found to be a more effective and efficient catalyst for reduction of 4-nitrophenol and 4-nitroaniline as compared to nitrobenzene.

Key words: Microgels, hybrid microgels, silver, nanoparticles, catalysis

1. Introduction

Plasmonic nanoparticles have gained a lot of attention over the last 20 years due to their unique properties different from the bulk material. Their size and shape dependent properties make them potential candidates for applications in sensing,[1] imaging,[2] biomedicine,[3] antibacterial activity,[4] and catalysis.[5] The use of metal nanoparticles in catalysis is going to increase day by day due to their high surface to volume ratio. Aggregation of metal nanoparticles reduces surface to volume ratio and restricts their use in catalysis. Surfactants,[4] block copolymers,[6] dendrimers,[7] and microgels[8] are used as stabilizing agents to protect nanoparticles from aggregation. Smart polymer microgels are superior to other stabilizing agents due to their unique combination of responsive and electronic properties of organic and inorganic materials respectively. Metal nanoparticles are synthesized inside the microgel network by in situ reduction.[9] In this way, size, size distribution, surface to volume ratio, and optical properties of metal nanoparticles can be controlled by adjusting the ratio of cross-linker content and monomer content during the synthesis of microgels.[10]

*Correspondence: zhfarooqi@gmail.com

Metal nanoparticles are stabilized inside the microgels for a long time due to the interaction of metal nanoparticles with pendant groups of microgels and the mechanical barrier of the polymer network around the nanoparticles.[11] The catalytic activity of hybrid microgels can be tuned by changing external stimuli like temperature.[12] The reactant molecules can reach metal nanoparticles through the open network of microgels. This open network also facilitates the diffusion of products formed from the surface of metal nanoparticles to outside the network. The hybrid microgels can be separated from the reaction mixture after completion of the reaction by simple methods like centrifugation and ultrafiltration. Due to these advantages, catalysis by hybrid microgels has gained a lot of attention in current research.[13] Scientists are continuously using hybrid microgels as catalysts for degradation of toxic chemicals. For example, Lui et al. reported the catalytic reduction of 4-nitrophenol (4-NP) in aqueous medium using silver (Ag) nanoparticles fabricated poly(N-isopropylacrylamide) hybrid microgels and showed that the catalytic activity can be tuned by varying temperature from 20 to 45 °C.[14] Zhang et al. designed a responsive polymer microgel system using N-isopropylacrylamide and chitosan derivatives for the fabrication of Ag nanoparticles.[15] They used this hybrid system for catalytic degradation of 4-NP. They showed that the catalytic activity of hybrid microgels can be tuned by swelling and deswelling of microgels under variation of external stimuli.

We have recently reported the catalytic activity of Ag nanoparticles fabricated in poly(N-isopropylacrylamide-co-methacrylic acid) [p(NIPAM-co-MAAc)],[16] poly(N-isopropylacrylamide-co-acrylic acid) [p(NIPAM-co-AAc)],[10,17] and poly(N-isopropylacrylamide-co-methacrylic acid-co-acrylamide) [p(NIPAM-co-MAAc-co-AAm)][18] microgels for catalytic applications. The effect of catalyst dosage on reduction of 4-NP was studied by using Ag nanoparticles fabricated p(NIPAM-co-MAAc) microgels as catalyst.[16] We have reported the effect of temperature on catalytic activity of Ag-p(NIPAM-co-MAAc-co-AAm) hybrid microgels.[18] We have also investigated the effect of the mole percentage of crosslinker on the size of nanoparticles and catalytic activity of Ag-p(NIPAM-co-AAc) hybrid microgels.[10] We recently published the effect of mole percentage of ionic monomer on size of nanoparticles and catalytic activity of Ag-p(NIPAM-co-AAc) hybrid microgels.[17] In continuation of this work, herein we report a new microgel system containing NIPAM and AAAc fabricated with Ag nanoparticles for catalytic reduction of different nitroarenes in aqueous medium.

To the best of our knowledge, there is no report in the literature on the fabrication of Ag nanoparticles in poly(N-isopropylacrylamide-co-allylacetic acid) [p(NIPAM-co-AAAc)] microgels for catalytic applications.

We prepared p(NIPAM-co-AAAc) microgels for synthesis of Ag nanoparticles inside the network. The hybrid material was characterized by ultraviolet-visible spectroscopy, Fourier transform infrared spectroscopy (FTIR), X-ray diffraction spectroscopy (XRD), transmission electron microscopy (TEM), and dynamic light scattering (DLS). This hybrid microgel was used as catalyst for reduction of 4-NP, 4-nitroaniline (4-NA), and nitrobenzene (NB) in aqueous medium. The catalytic activity of the hybrid system for 4-NP, 4-NA, and NB was compared in this study.

2. Results and discussion

2.1. Synthesis of p(NIPAM-co-AAAc) microgels

Normally, totally cross-linked microgel structures are synthesized by free radical emulsion polymerization or precipitation polymerization or solution polymerization. Here, p(NIPAM-co-AAAc) microgels were synthesized using free radical emulsion polymerization in aqueous medium. Chemical and physical interactions are involved in the synthesis of microgels.[19]

NIPAM-based microgels having allylacetic acid as comonomer was synthesized. Polymerization was carried out under continuous nitrogen purge to remove surface oxygen; otherwise oxidation of free radicals occurred.[20] Polymerization at high temperature is advantageous because it causes formation of sulfate radicals by decomposition of APS, which initiates polymerization. After initiation, the NIPAM monomers are polymerized and the chain starts to grow. After attaining a certain critical length it starts breaking and precipitating into precursor particles. The precursor particles are unstable and so they tend to grow either by aggregating with already present precursor particles or by existing colloidally stable particles. The charge conveyed by the initiator to stabilize the precursor particles is not sufficient and so surfactant is added. It not only stabilizes precursor particles but also gives microgels in nanometer range.[18,21] After the polymerization process, the color of the solution was found to change from transparent to milky, which indicated the formation of microgels. Light scattering of microgels was found to change with the changing dimensions of microgels, which appeared as change in the color of microgel.[22]

The number of moles of AAAc was kept low as compared to NIPAM in the feed composition of the microgels because it has been reported previously that an increase in the mole ratio of ionic monomer to NIPAM in the feed composition of copolymer microgels increases the possibility of homopolymer-ization instead of copolymer-ization and decreases the ratio of contents of AAAc to NIPAM incorporated in the microgels.[23] AAAc content incorporated within p(NIPAM-co-AAAc) microgels was found to be 1.5 mol %. This amount is much smaller than that of feed mol % of AAAc because AAAc does not polymerize easily.

2.2. In situ synthesis of silver nanoparticles in p(NIPAM-co-AAAc) microgels

Ag-p(NIPAM-co-AAAc) hybrid microgels have been synthesized by reduction of silver ions (Ag^+) within the network of microgel.[10] For the diffusion of maximum silver ions within the network of microgel and to ensure deprotonation of carboxyl groups, the pH of the reaction mixture was kept greater than pK_a (4.51) of AAAc. On addition of silver nitrate solution at high pH, anion exchange occurs between the polymer microgel and water aqueous salt solution. Silver ions move towards carboxylate ions due to electrostatic attractions and are fixed in the microgel network by making ionic bonds with carboxylate ions. $NaBH_4$ reduces these fixed silver ions and converts them into monoatomic silver. Monoatomic silver aggregates to form nanoparticles within sieves of the microgel network; hence reduction occurs in the whole network of the microgel.[17] Therefore, microgels not only act as microreactor for nanoparticle synthesis but also provide stability to nanoparticles. The golden-yellow dispersion formation after addition of $NaBH_4$ was due to formation of Ag nanoparticles. Content of Ag loaded within microgels was found to be equal to 2.91×10^{-3} mol per gram of p(NIPAM-co-AAAc) microgels. This amount is almost equal to the feed content of Ag per gram of microgels. It means that chemical reduction is an efficient method for in situ synthesis of Ag nanoparticles. Ag nanoparticles were found to be stable within p(NIPAM-co-AAAc) microgels for a long time. That is why p(NIPAM-co-AAAc) is said to be a suitable carrier for Ag nanoparticles and their catalytic applications. Moreover, the open network of microgels at high pH offers less hindrance against diffusion of nitroarenes and borohydride ions (as supported by the DLS study of section 2.7).

2.3. UV-visible spectra of p(NIPAM-co-AAAc) microgels and Ag-p(NIPAM-co-AAAc) hybrid microgels

UV-visible absorption spectra of the pure p(NIPAM-co-AAAc) microgel and Ag- p(NIPAM-co-AAAc) hybrid microgel are shown in Figure 1. The Ag-p(NIPAM-co-AAAc) hybrid microgels showed a sharp absorption band

at around 411 nm, which indicates the formation of Ag nanoparticles.[24] The single and sharp absorption band in the UV-visible spectra of the hybrid microgels indicates that synthesized Ag nanoparticles are spherical with a narrow size distribution.[24] However, pure p(NIPAM-co-AAAc) microgel does not show any such peak because pure microgels are devoid of nanoparticles.

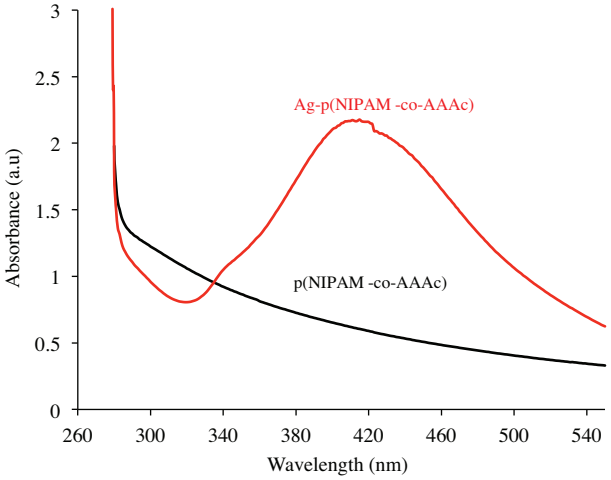

Figure 1. UV-visible spectra of pure p(NIPAM-co-AAAc) microgels and Ag-p(NIPAM-co-AAc) hybrid microgels at 31 °C.

2.4. FTIR analysis of pure and hybrid microgels

Figure 2 shows the FTIR spectra of p(NIPAM-co-AAAc) microgel and Ag-p(NIPAM-co-AAAc) hybrid microgel. The values of absorption bands of different functional groups are listed in Table 1. Figure 2 and Table 1 show that NIPAM and AAAc are incorporated within the polymer microgels and hybrid microgels because absorption bands of their bonds are present in their spectra. No absorption band of the carbon–carbon double bond ($\sim$1600 cm^{-1}) is present in the FTIR spectra. This indicates that no unreacted monomer is present in samples of microgels and hybrid microgels.[17] The spectra in Figure 2 are similar, which shows that fabrication of nanoparticles does not alter the bonds of the polymer. However, due to the interaction between the carbonyl group and nanoparticles, the absorption band of the carbonyl group becomes sharper in hybrid microgels as compared to that in pure microgels. FTIR spectroscopy has been used by Farooqi et al. to confirm the structure of microgels.[10]

Table 1. Values of absorption bands of various chemical bonds of p(NIPAM-co-AAAc) microgels and Ag-p(NIPAM-co-AAAc) hybrid microgels.

Chemical bond	Mode of vibration	Functional group	Observed absorption band (cm^{-1})	
			p(NIPAM-co-AAAc)	Ag-p(NIPAM-co-AAAc)
N–H	Stretching	Amine	3277	3332
O–H	Stretching	Carboxyl	3050	3050
CH_3	Stretching	Alkyl	2971	2974
C=O	Stretching	Carbonyl	1523	1655
N–H	Bending	Amine	1530	1541
C–O	Stretching	Carboxyl	1459	1459
CH_2	Bending	Alkane	1399	1342

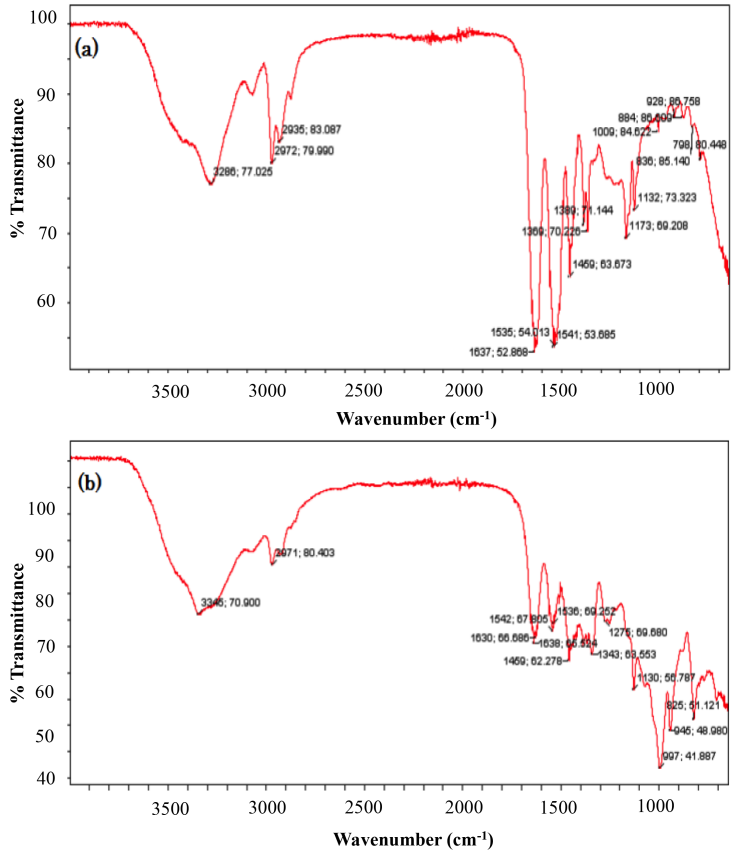

Figure 2. FTIR spectra of (a) p(NIPAM-co-AAAc) microgels and (b) Ag-p(NIPAM-co-AAAc) hybrid microgels.

2.5. TEM analysis of Ag-p(NIPAM-co-AAAc) hybrid microgels

The TEM image of the Ag-p(NIPAM-co-AAAc) hybrid microgels is shown in Figure 3. It is clear from the figure that Ag nanoparticles fabricated in p(NIPAM-co-AAAc) microgels are spherical as supported by the UV-visible spectra shown in Figure 1. The TEM image shows that Ag nanoparticles were stable inside the microgel network for a long time because the TEM image of the hybrid microgels was taken after 8 months of synthesis. The diameter of the Ag nanoparticles was in the range of 20–40 nm.

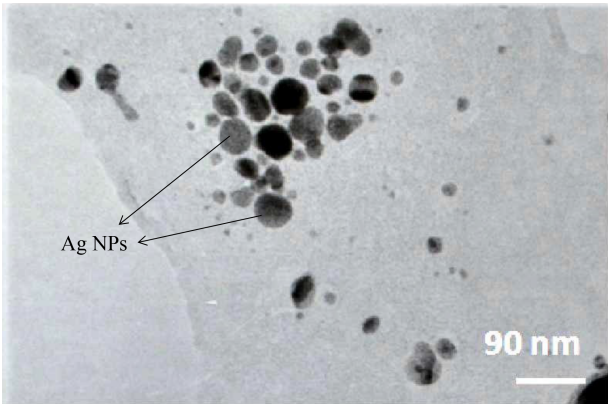

Figure 3. TEM image of Ag nanoparticles fabricated in p(NIPAM-co-AAAc) microgels.

2.6. XRD analysis of Ag-p(NIPAM-co-AAAc) hybrid microgels

The crystalline structure of Ag nanoparticles present in the p(NIPAM-co-AAAc) microgels was investigated by XRD. Figure 4 gives the XRD pattern of the Ag-p(NIPAM-co-AAAc) hybrid microgels, which exhibit a characteristic peak at the scattering angle (2 θ) of 26.165°. This shows that the hybrid microgels are crystalline in nature.

2.7. DLS analysis of p(NIPAM-co-AAAc) microgels

DLS was employed to study the temperature and pH sensitivity of the p(NIPAM-co-AAAc) microgels.

2.7.1. Temperature sensitivity of p(NIPAM-co-AAAc) microgels

The hydrodynamic radius (R_h) of p(NIPAM-co-AAAc) microgels was found to decrease with an increase in temperature from 15 to 36 °C. The decrease in radius with an increase in temperature is attributed to shrinking of p(NIPAM-co-AAAc) microgels. At low temperature microgels are in swollen state. With increasing temperature hydrophilic interactions (present between water molecules and carboxyl groups of polymers) become weaker and eject water from the microgels, leading to microgel shrinking.[9] This shrinking occurred up to 36 °C. Above this temperature microgels become aggregated as shown by Figure 5. This aggregation leads to an increase in R_h with an increase in temperature (Figure 5). The temperature responsive behavior of p(NIPAM-co-AAAc) microgels at pH 8 is different from that of p(NIPAM-co-AAc) and p(NIPAM-co-MAAc) under the same conditions.[25–27] The p(NIPAM-co-AAc)[28] and p(NIPAM-co-MAAc)[29] are found to stable at pH $\geq$ 8 in aqueous medium under the wide range of temperature (from 15 to 50 °C) but p(NIPAM-co-AAAc) microgels show aggregation at T $\geq$ 36 °C in aqueous medium, which is due to the more hydrophobic nature of AAAc as compared to AAc and MAAc.

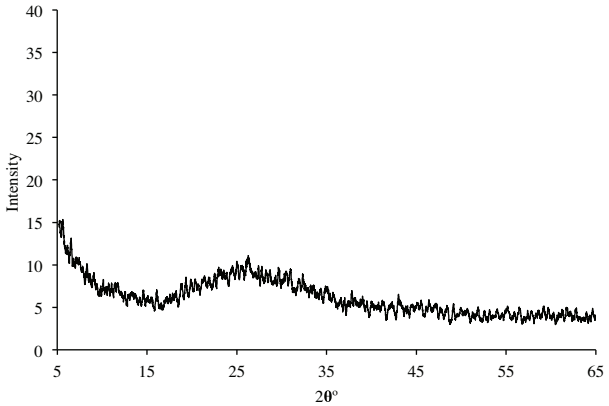

Figure 4. XRD pattern of Ag-p(NIPAM-co-AAAc) hybrid microgels.

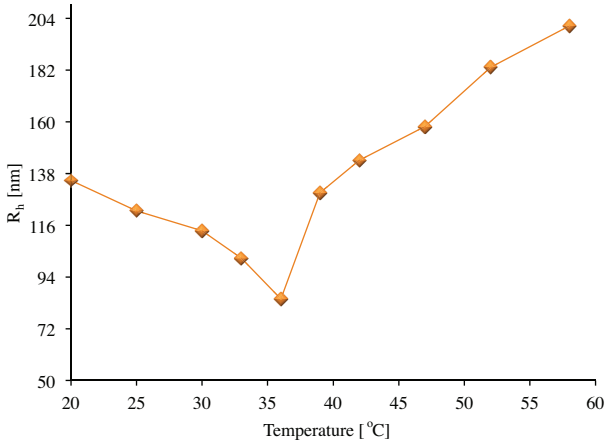

Figure 5. Temperature sensitivity of p(NIPAM-co-AAAc) microgels at pH 8.

2.7.2. pH sensitivity of p(NIPAM-co-AAAc) microgels

The R_h of p(NIPAM-co-AAAc) microgels as a function of pH of the medium at 27 °C is shown in Figure 6. The value of R_h increases with an increase in the pH of the medium due to deprotonation of carboxyl groups of

AAAc units present in the network of microgels. The electrostatic repulsion between carboxylate ions present in the network causes swelling in the microgel particles. It also increases the hydrophilicity of the network and water moves from outside to inside the network, due to which the size of microgel particles increases as shown in Figure 6. The important feature of pH sensitivity of p(NIPAM-co-AAAc) microgels is that Ag^+ can be entrapped inside the network due to electrostatic attraction between Ag^+ and carboxylate groups. At high pH, the microgel particles exist in swollen state, which facilitates the diffusion of reactant molecules towards the catalyst surface. That is why reduction of nitroarenes was carried out at room temperature and high pH.

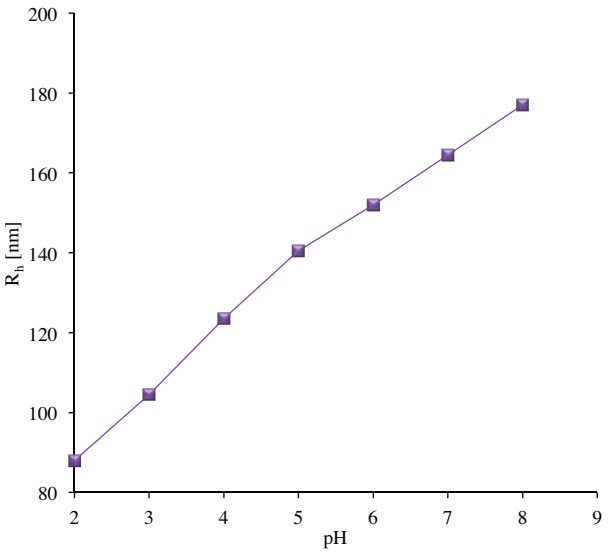

Figure 6. pH sensitivity of p(NIPAM-co-AAAc) microgels at temperature 27 °C.

2.8. Study of catalytic reduction of nitroarenes by UV-visible spectroscopy

Ag-p(NIPAM-co-AAAc) hybrid microgels were used as catalyst for reduction of NB, 4-NA, and 4-NP in aqueous medium. The reduction was carried out under the same conditions of concentration of nitroarene, $NaBH_4$, and catalyst dosage at 27 °C for comparative study of reaction rates. The progress of the reduction reaction was monitored by UV-visible spectrophotometry. The time dependent spectra for reduction of NB, 4-NA, and 4-NP are shown in Figures 7–9, respectively.

Upon reduction, NB is converted into aniline (AB) by $NaBH_4$ in the presence of Ag-p(NIPAM-co-AAAc) hybrid microgels. NB and AB both absorb in the UV range at 268 and 230 nm, respectively. As the reaction progresses absorbance at 268 nm decreases with the passage of time and absorbance at 230 nm increases (Figure 7). An isosbestic point at 243 nm appears in the time dependent UV spectra in Figure 7, which shows that AB is the only UV absorbing product of reduction. λ_{max} of NB slightly red shifts to 275 nm along with the progress of the reaction. This peak shifting is due to formation of AB in the reaction mixture because AB slightly absorbs at 275 nm.

Figure 8 shows the UV spectra of the catalytic reduction of 4-NA into 4-aminoaniline (4-AA). 4-NA absorbs at 380 nm while 4-AA absorbs at 240 nm in the UV range. With the progress of the reaction, absorbance at 380 nm decreases along with a concomitant increase in absorbance at 240 nm, indicating that concentration of 4-NA decreases with the passage of time and concentration of 4-AA increases with the passage of time. The UV spectra of the catalytic reduction of 4-NA possess an isosbestic point at 303 nm.

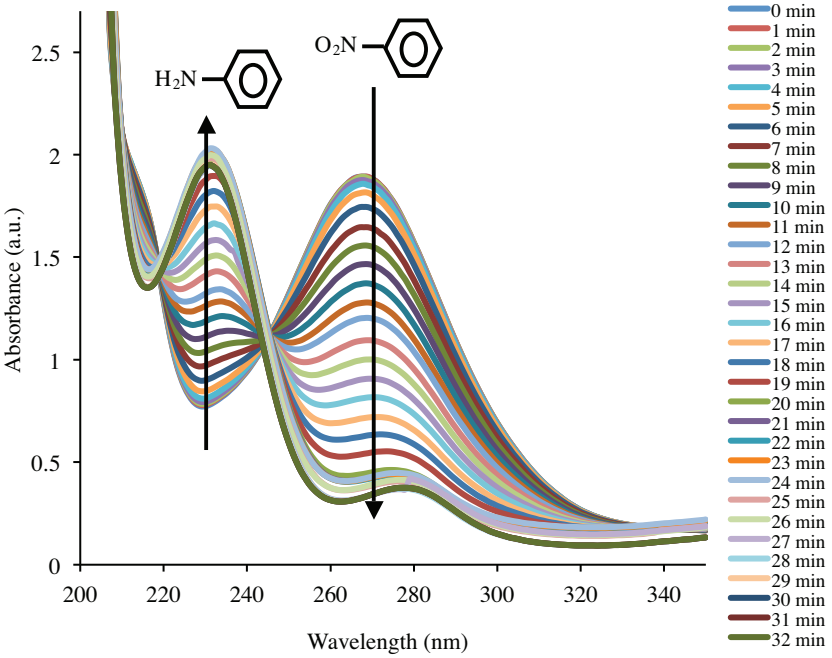

Figure 7. UV spectra of reduction of NB by Ag-(NIPAM-co-AAAc) hybrid microgels at 27 °C.

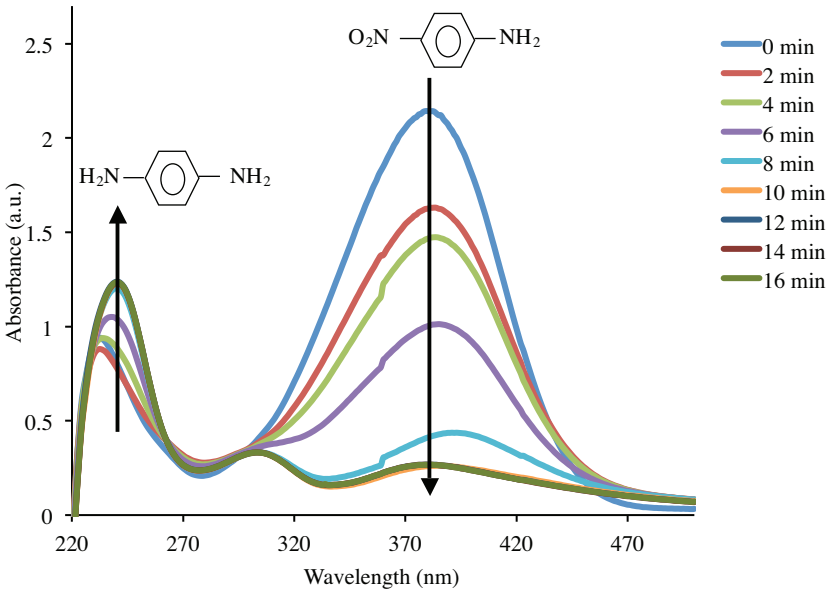

Figure 8. UV spectra of reduction of 4-NA by Ag-p(NIPAM-co-AAAc) hybrid microgels at 27 °C.

The UV-visible spectra of the catalytic reduction of 4-NP into 4-aminophenol (4-AP) are shown in Figure 9. λ_{max} of 4-NP is 400 nm while that of 4-AP is 300 nm. One characteristic peak at 400 nm is present in this figure at 0 min, which indicates that 4-NP is present in the reaction mixture. As the reaction progresses absorbance at 300 nm increases and absorbance at 400 nm decreases, which shows that 4-NP is converting into 4-AP. When absorbance at 400 and 300 nm become constant it shows that the reaction is complete.

Catalytic reduction of NB, 4-NA, and 4-NP was studied by using $NaBH_4$ in excess. Thus the reaction was supposed to be pseudo first order with respect to concentration of nitroarene. Eq. (1) was used to determine

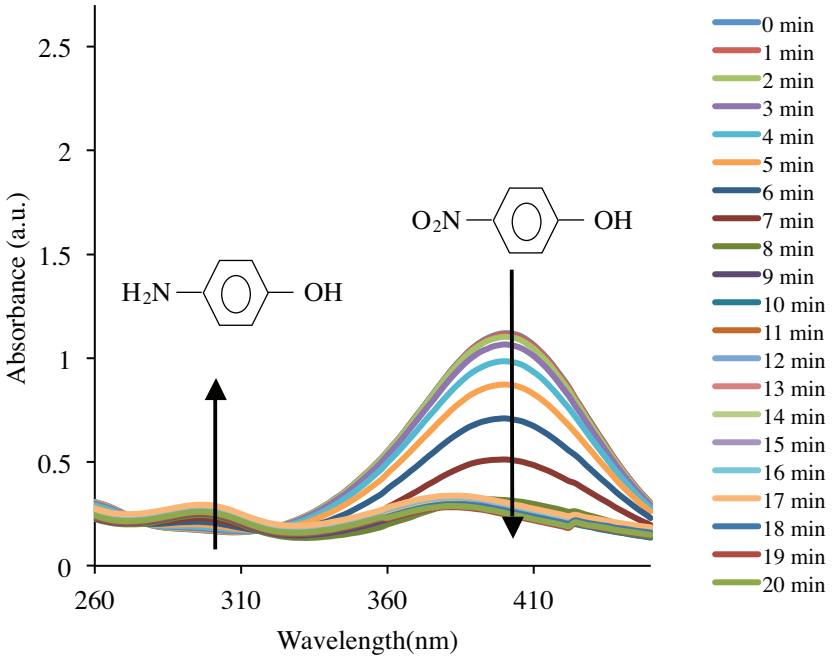

Figure 9. UV-visible spectra of reduction of 4-NP by Ag-(NIPAM-co-AAAc)hybrid microgels at 27 °C.

the value of k_{app} of reduction.

$$\ln\left(A_t/A_o\right) = -k_{app}\,t, \tag{1}$$

where A_o is the absorbance of nitroarene at 0 min and A_t is absorbance of nitroarene at time t.

Plots of ln (A_t/A_o) as a function of time for reduction of NB, 4-NA, and 4-NP are shown in Figure 10. Values of k_{app} calculated from the slopes of these plots are 0.089, 0.215, and 0.248 min^{-1} for NB, 4-NA, and 4-NP, respectively. Initially the value of ln (A_t/A_o) does not change with the passage of time for all nitroarenes, which shows that reduction has not started yet. This time duration is called the induction period. The induction periods for NB, 4-NA, and 4-NP are 5, 0, and 9 min, respectively. Many important phenomena like diffusion of reactants and adsorption of reactants on the surface of nanoparticles occur during this period. After the induction period, the value of ln (A_t/A_o) decreases with the passage of time, indicating that the reaction is in progress. This linear region of plots was used to calculate the value of k_{app}. When the reaction is complete the value of ln (A_t/A_o) again becomes constant with the passage of time.

The comparative study of the rate of reduction of nitroarenes showed the following order of reactivity: NB < 4-NA < 4-NP (Table 2). The reaction progress times of the catalytic reduction of NB, 4-NA, and 4-NP are 15, 10, and 7 min respectively. This shows that the catalytic reduction of NB is slower as compared to that of 4-NA and 4-NP. NB is less hydrophilic as compared to 4-NA and 4-NP. 4-NA and 4-NP possess hydroxyl and amino hydrophilic functional groups, respectively. These groups make 4-NA and 4-NP more hydrophilic as compared to NB.[30] Microgels are hydrophilic at 27 °C in basic medium (as indicated by the DLS study of section 2.7) and catalysis is also studied under the same conditions. Therefore, hydrophilic 4-NA and 4-NP are attracted towards microgels and rapidly diffuse towards nanoparticles through the network of microgels compared to NB, and increase the value of k_{app} of reduction of 4-NA and 4-NP as compared to that of NB. These results are found to be in agreement with the results obtained by Pradhan et al.[31] and Shin and Huh.[32]

That is why hydrophilic system conditions have proved to be favorable for catalytic reduction of 4-NP and 4-NA. Cobalt-poly(N-isopropylacryl amide-co-methacrylic acid) [Co-p(NIPAM-co-MAAc)] and nickel-poly(N-isopropylacryl amide-co-methacrylic acid) [Ni-p(NIPAM-co-MAAc)] hybrid microgels for catalytic reduction of 4-NP under similar conditions have been reported by our group.[8] The reported value of k_{app} for catalytic reduction of 4-NP was a little smaller than that observed in this work. Ajmal et al. have also reported catalytic reduction by Ni, Co, and copper (Cu) nanoparticles stabilized with poly(methacrylic acid) [p(MAAc)].[33] Under similar conditions, the values of k_{app} reported by them are greater than that observed in this work. However, Co, Cu, and Ni nanoparticles are not stable for a long time. Ag-p(NIPAM-co-AAAc) hybrid microgels are found to be stable for 6 months. No shift in surface plasmon band was observed in the UV-visible spectra of the hybrid microgels after 6 months.

Table 2. The values of k_{app} and reaction progress time of catalytic reduction of NB, 4-NA, and 4-NP in aqueous medium at 27 °C using Ag-p(NIPAM-co-AAAc) hybrid microgels as catalyst.

Nitroarene	k_{app} (min^{-1})	Reaction progress time (min)
NB	0.089	15
4-NA	0.215	10
4-NP	0.248	7

Moreover, the recycling ability of Ag-p(NIPAM-co-AAAc) hybrid microgels was measured in terms of percentage activity of the catalyst on four repeated uses of it for the catalytic reduction of 4-NP under constant reaction conditions. The percentage activity was calculated by dividing the value of the rate constant for the second, third, and fourth uses to that for the first use and multiplying the answer by a hundred. The data are shown in Figure 11. The slight decrease in the percentage may be due to oxide layer formation around the nanoparticles.

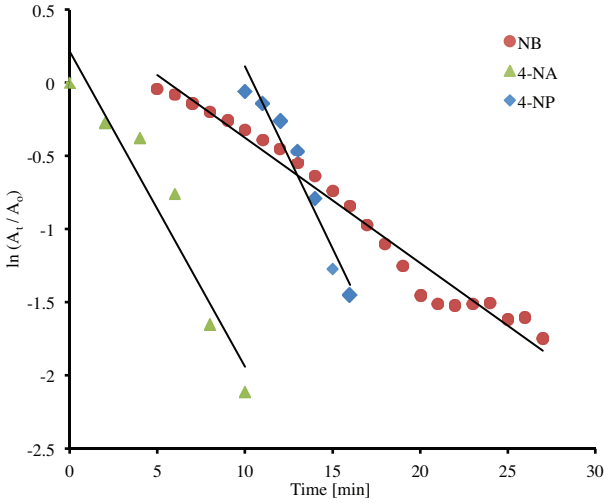

Figure 10. Plot of ln (A_t/A_o) versus time for reduction of NB, 4-NP, and 4-NA by Ag-p(NIPAM-co-AAAc) hybrid microgels at 27 °C.

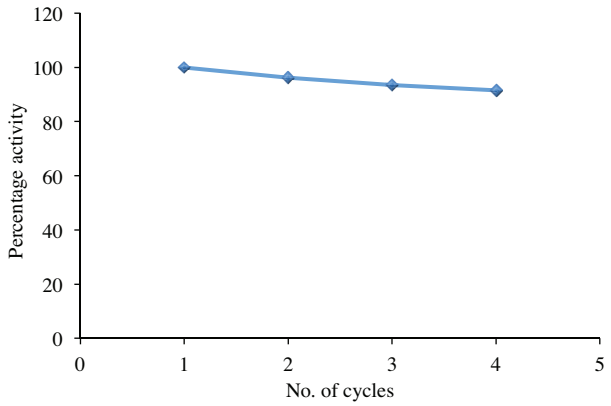

Figure 11. Percentage activity of Ag-p(NIPAM-co-AAAc) hybrid microgels as a function of number of cycles for catalytic reduction of 4-NP in aqueous medium.

3. Materials and methods

3.1. Materials

N-isopropylacrylamide (NIPAM), N,N-methylenebisacrylamide (BIS), sodium dodecylsulfate (SDS), ammonium persulfate (APS), nitrobenzene (NB), and 4-nitrophenol (4-NP) were bought from Sigma-Aldrich (Germany). Allyl acetic acid (AAAc) and 4-nitroaniline (4-NA) were bought from Acros Organics and Merck Schuchardt, respectively. Sodium borohydride ($NaBH_4$) was of synthetic grade purchased from Scharlau Company (Australia). Silver nitrate ($AgNO_3$) was bought from Germiston Chemicals. Deionized water was used for solution preparation throughout the experimental work. The dialysis membrane used for purification of the microgels was Spectra/Por molecular porous membrane tubing (Fisher Scientific) having MWCO of 12,000–14,000.

3.2. Synthesis of p(NIPAM-co-AAAc) microgels

The microgels were prepared by free-radical emulsion polymerization of NIPAM and AAAc monomers as previously reported by our group.[34,35] BIS, APS, and SDS were used as cross-linker, initiator, and emulsifying agent, respectively. The reaction mixture having 0.255 g of NIPAM, 0.0193 g of BIS, 0.05 g of SDS, and 95 mL of deionized water was taken in a round bottom flask equipped with a thermometer, condenser, stirrer, and nitrogen gas inlet. The mixture was stirred at room temperature to dissolve the components. When it became clear, 13 μL of AAAc was added to it. The mixture was heated up to 70 °C under continuous nitrogen purge. After 30 min, 5 mL of freshly prepared 0.05 M APS solution was added. The reaction was allowed to proceed for 5 h under continuous nitrogen purge, maintaining the temperature at 70 °C throughout the reaction. A turbid white colloidal solution was obtained at the end of the reaction, indicating the formation of microgel. The microgel was cooled to room temperature (21 °C) and purified by dialysis for 6 days with constant stirring at room temperature. Dialysis was carried out to remove the surfactant and unreacted monomers. Content of AAAc incorporated within the microgels was determined by titration with 0.01 M sodium hydroxide using the method reported previously.[36]

3.3. In situ synthesis of silver nanoparticles within p(NIPAM-co-AAAc) microgels

Ag-p(NIPAM-co-AAAc) hybrid microgels were prepared by in situ reduction of $AgNO_3$ within the network of microgels. First 6 mL of the as-prepared p(NIPAM-co-AAAc) microgels and 38.85 mL of deionized water were taken in a 250-mL three-necked round bottom flask, equipped with a condenser, a thermometer, stirrer and nitrogen gas inlet. pH of the reaction mixture was checked using a pH meter and was observed to be 6. Then 0.15 mL of 0.1 M $AgNO_3$ was added to the reaction mixture. The mixture was stirred for 30 min under nitrogen purge. Next 0.01 g of $NaBH_4$ was dissolved in 5 mL of deionized water and then added to the reaction mixture dropwise. The mixture was again stirred for 2 h. The hybrid microgels were cooled at room temperature (21 °C) and purified by dialysis using Spectra/Por molecular porous membrane tubing against changed fresh water. Then a sample of hybrid microgels was digested by 5 M hydrochloric acid and content of Ag was analyzed by using an atomic absorption spectrophotometer.

3.4. Catalytic reduction of nitroarenes

Ag-p(NIPAM-co-AAAc) hybrid microgels were used as catalyst for reduction of 4-NP, 4-NA, and NB in aqueous medium. First 1.8 mL of 0.1 mM nitroarene solution and 0.2 mL of hybrid microgels containing 6.78 μg of Ag content were taken in a cuvette. Next 0.5 mL of 45 mM $NaBH_4$ was added and the UV-visible spectrum was

recorded at regular time intervals until completion of the reduction. To check the recycling ability, the hybrid microgels were collected by decantation after completion of the catalytic reduction of 4-NP. The catalyst was washed with deionized water in order to reuse it for the same reaction under the same conditions.

3.5. Characterization

A Labomed Inc. UVD-3500 double beam spectrophotometer ranging from 200 to 1100 nm was used for the study of the catalytic activity of Ag-p(NIPAM-co-AAAc) hybrid microgel for different nitroarenes. The FTIR spectra of oven-dried microgel and hybrid microgel samples were recorded on a Cary 630 FTIR spectrophotometer (Agilient Technology, USA). The TEM image of the air-dried hybrid microgel sample was taken on a FESEM JSM-7500 F (JEOL Limited, USA) equipped with transmission detectors operated at 80 kV. Powder XRD patterns of hybrid microgels were recorded on an X-PERT PRO diffractometer containing CuKα source and working at 40 kV and 40 mA. The DLS study was carried out by BI-200 SM (Brookhaven Instruments Corp., USA) at an angle of 90° equipped with a standard He–Ne laser (632.8 nm). A Cp-409 pH meter manufactured by Elmeiron Company was used for pH measurement. Content of Ag was analyzed by flame atomic absorption spectrophotometer (AAnalyst 100, PerkinElmer, USA).

4. Conclusions

p(NIPAM-co-AAAc) microgels were synthesized using NIPAM as monomer and allylacetic acid as comonomer by free radical emulsion polymerization. These microgels were used as microreactor to fabricate Ag nanoparticles inside the polymer network. Ag nanoparticles of spherical shape with average diameter of 20–40 nm were successfully stabilized in p(NIPAM-co-AAAc) microgels for a long time. A comparative study of the catalytic activity of Ag-p(NIPAM-co-AAAc) hybrid microgels by reduction of nitroarenes to their respective amino-arenes was performed in the presence of excess $NaBH_4$. The reduction reactions were found to be first order with respect to nitroarenes with the values of apparent rate constants (k_{app}) equal to 0.248, 0.215, and 0.089 min^{-1} for 4-nitrophenol, 4-nitroaniline, and nitrobenzene at 27 °C, respectively. Silver nanoparticles were found to be a more effective and efficient catalyst for reduction of 4-nitrophenol and 4-nitroaniline than nitrobenzene. This may be attributed to the faster adsorption and diffusion of hydrophilic 4-nitrophenol and 4-nitroaniline than hydrophobic nitrobenzene on hydrophilic microgel's surface. This hybrid system has the potential to be used as an effective catalyst for reduction of other aromatic nitro compounds in aqueous medium. Moreover, the catalyst can be recycled for repeated use with no significant decrease in percentage catalytic activity.

Acknowledgment

The authors are grateful to the University of the Punjab, Lahore, Pakistan, for financial support under research grant for the fiscal year 2014–2015.

References

1. Cobley, C.; Skrabalak, S.; Campbell, D.; Xia, Y. *Plasmonics* **2009**, *4*, 171–179.
2. Gierden, A.; Sanchez, W.; Zvyagin, A. V.; Zhao, X.; Ross, J. A.; Roberts, M. S. *J. Biomed. Opt.* **2008**, *13*, 64031–64039.
3. Pankhurst, Q. A.; Connolly, J.; Jones, S.; Dobson, J. *J. Phys. D: Appl. Phys.* **2003**, *36*, 167–178.
4. Kvitek, L.; Panácek, A.; Soukupova, J.; Kolar, M.; Vecerova, R.; Prucek, R.; Holecová, M.; Zboril, R. *J. Phys. Chem. C* **2008**, *112*, 5825–5834.

5. Alonso, F.; Moglie, Y.; Radivoy, G.; Yus, M. *Tetrahedron Lett.* **2009**, *50*, 2358–2362.
6. Qi, L.; Cölfen, H.; Antonietti, M. *Nano Lett.* **2001**, *1*, 61–65.
7. Antonels, N. C.; Meijboom, R. *Langmuir* **2013**, *29*, 13433–13442.
8. Farooqi, Z. H.; Iqbal, S.; Khan, S. R.; Kanwal, F.; Begum, R. *e-Polymers* **2014**, *14*, 313–321.
9. Naeem, H.; Farooqi, Z. H.; Shah, L. A.; Siddiq, M. *J. Polym. Res.* **2012**, *19*, 1–10.
10. Farooqi, Z. H.; Khan, S. R.; Hussain, T.; Begum, R.; Ejaz, K.; Majeed, S.; Ajmal, M.; Kanwal, F.; Siddiq, M. *Korean J. Chem. Eng.* **2014**, *31*, 1674–1680.
11. Farooqi, Z. H.; Siddiq, M. *J. Disp. Sci. Technol.* **2015**, *36*, 423–429.
12. Dong, Y.; Ma, Y.; Zhai, T.; Zeng, Y.; Fu, H.; Yao, J. *J. Nanosci. Nanotechnol.* **2008**, *8*, 6283–6289.
13. Agrawal, G.; Schürings, M. P.; van Rijn, P.; Pich, A. *J. Mater. Chem. A* **2013**, *1*, 13244–13251.
14. Liu, Y. Y.; Liu, X. Y.; Yang, J. M.; Lin, D. L.; Chen, X.; Zha, L. S. *Colloid Surface. A* **2012**, *393*, 105–110.
15. Zhang, J. T.; Wei, G.; Keller, T. F.; Gallagher, H.; Stötzel, C.; Müller, F. A.; Gottschaldt, M.; Schubert, U. S.; Jandt, K. D. *Macromol. Mater. Eng.* **2010**, *295*, 1049–1057.
16. Khan, S. R.; Farooqi, Z. H.; Ajmal, M.; Siddiq, M.; Khan, A. *J. Disp. Sci. Technol.* **2013**, *34*, 1324–1333.
17. Farooqi, Z. H.; Khan, S. R.; Begum, R.; Kanwal, F.; Sharif, A.; Ahmed, E.; Majeed, S.; Ijaz, K.; Ijaz, A. *Turk. J. Chem.* **2015**, *39*, 96–107.
18. Ajmal, M.; Farooqi, Z. H.; Siddiq, M. *Korean J. Chem. Eng.* **2013**, *30*, 2030–2036.
19. Terashima, T. *Encyclopedia Polym. Sci. Technol.* **2013**, DOI: 10.1002/ 0471440264.pst590.
20. Karg, M.; Pastoriza-Santos, I.; Rodriguez-Gonzalez, B.; von Klitzing, R.; Wellert, S.; Hellweg, T. *Langmuir* **2008**, *24*, 6300–6306.
21. Al-Manasir, N.; Zhu, K.; Kjøniksen, A. L.; Knudsen, K. D.; Karlsson, G.; Nystrom, B. *J. Phys. Chem. B* **2009**, *113*, 11115–11123.
22. Zhang, J. T.; Liu, X. L.; Fahr, A.; Jandt, K. D. *Colloid Polym. Sci.* **2008**, *286*, 1209–1213.
23. Karg, M.; Pastoriza-Santos, I.; Rodriguez-Gonzalez, B.; von Klitzing, R.; Wellert, S.; Hellweg, T. *Langmuir* **2008**, *24*, 6300–6306.
24. Wu, W.; Zhou, T.; Zhou, S. *Chem. Mater.* **2009**, *21*, 2851–2861.
25. Farooqi, Z. H.; Khan, H. U.; Shah, S. M.; Siddiq, M. *Arabian J. Chem.* **2013**, DOI: 10.1016/j.arabjc.2013.07.031.
26. Xiong, W.; Gao, X.; Zhao, Y.; Xu, H.; Yang, X. *Colloids Surface. B* **2011**, *84*, 103–110.
27. Zhou, S.; Chu, B. *J. Phys. Chem. B* **1998**, *102*, 1364–1371.
28. Snowden, M. J.; Chowdhry, B. Z.; Vincent, B.; Morris, G. E. *J. Chem. Soc., Faraday Trans.* **1996**, *92*, 5013–5016.
29. Saunders, B. R.; Vincent, B. *Adv. Colloid Interface Sci.* **1999**, *80*, 1–25.
30. Sahiner, N.; Ozay, O.; Aktas, N. *Chemosphere* **2011**, *85*, 832–838.
31. Pradhan, N.; Pal, A.; Pal, T. *Colloids Surface. A* **2002**, *196*, 247–257.
32. Shin, H. S.; Huh, S. *ACS Appl. Mater. Interf.* **2012**, *4*, 6324–6331.
33. Ajmal, M.; Siddiq, M.; Al-Lohedan, H.; Sahiner, N. *RSC Advances.* **2014**, *4*, 59562–59570.
34. Farooqi, Z. H.; Wu, W.; Zhou, S.; Siddiq, M. *Macromol. Chem. Phys.* **2011**, *212*, 1510–1514.
35. Farooqi, Z. H.; Khan, A.; Siddiq, M. *Polym. Int.* **2011**, *60*, 1481–1486.
36. Christensen, M. L.; Keiding, K. *Colloids Surface. A* **2005**, *252*, 61–69.